Tuning the optical response of nanocylinder arrays: An analytical study

Marine Laroche,[1] Silvia Albaladejo,[1] Raquel Gómez-Medina,[2] and Juan José Sáenz[1]
[1]*Departamento de Física de la Materia Condensada and Instituto "Nicolás Cabrera," Universidad Autónoma de Madrid, E-28049 Madrid, Spain*[*]
[2]*Nanophotonics and Metrology Laboratory, Swiss Federal Institute of Technology, 1015 Lausanne, Switzerland*
(Received 6 October 2006; published 18 December 2006)

An analytical study of the optical properties of nanocylinder arrays is presented. The conditions to tune the absorption/thermal emission and extinction resonances of such systems are derived. We predict two kinds of resonances. Close to the Rayleigh anomalies, the array can generate quasimonochromatic and highly directional thermal emission/absorption. Isotropic emission/absorption can also be obtained when the material exhibits an absorption line or in the presence of localized surface plasmon/polaritons. For *s* polarization our analysis predicts a theoretical limit of 50% of absorption. Interestingly, for *p*-polarized light, a nanocylinder array can present perfect (100%) absorption.

DOI: 10.1103/PhysRevB.74.245422 PACS number(s): 78.67.−n, 42.25.Bs, 42.79.Dj, 73.20.Mf

I. INTRODUCTION

Understanding the absorption and thermal emission of electromagnetic radiation in nanostructured systems is a key issue in nanoscience and technology. Emission and absorption processes, closely connected from the well known Kirchhoff's law,[1] are of considerable interest in very different applications. Tailoring the thermal emission is specially relevant for thermophotovoltaic (TPV) applications and for the design of efficient light and infrared sources. For instance, photonic crystals and nanoparticle arrays can be used as efficient selective emitters.[2–5] Thermal antennas based on the excitation of surface waves[5–7] may also be used to produce quasimonochromatic and highly directional emission. On the other hand, controlling the absorption and extinction spectra of nanoparticles arrays[8–11] have drawn much attention recently for their potential applications to chemical and biological sensors as well as for surface enhanced Raman scattering (SERS).[12–14]

Most of the interesting optical properties of these nanostructured systems, obtained from experiments or numerical calculations, are usually attributed to the excitation of localized surface states,[5] plasmon/phonon-polariton resonances (SPR)[6,8–11] or guided modes[15] that are subsequently diffracted with some micro/nanostructured lattice periodicity. This point of view limits further developments to materials that support surface modes or complex photonic crystal structures supporting surface states. Moreover, due to the absence of simple analytical results, the optimization of the structure and materials for specific applications is a formidable task.

In this article, we show that a simple subwavelength cylinder array can be tuned to present striking emission and absorption characteristics. This system, which resembles a nanowire toaster grille, presents two different kinds of emission/absorption resonances. Close to the Rayleigh anomalies, the diffractive coupling with the lattice periodicity can generate coherent, quasimonochromatic and highly directional, thermal emission/absorption even in absence of any material or surface plasmon/polariton resonance. These *geometric* resonances lead to sharp peaks in the extinction spectra with characteristic Fano line shapes. Another kind of absorption resonances, with wider and symmetric line shapes, appears when the material exhibits an absorption line or in the presence of localized SPRs. At the resonant wavelength, the emission is isotropic which may be important for TPV applications. We analytically derive the conditions for resonant emission/absorption as a function of the geometry and material's parameters. We will demonstrate that for *s* polarization there is a theoretical limit of 50% of absorption. Interestingly, we will show that, for *p*-polarized light and an appropriate choice of parameters, an array of nanocylinders can present perfect (100%) absorption.

II. ANALYTICAL STUDY FOR *s* POLARIZATION

Let us consider an infinite set of parallel cylinders with their axis along the z axis (see inset in Fig. 1), relative dielectric constant $\epsilon=\epsilon'+i\epsilon''$ and radius a much smaller than the wavelength. The cylinders are located at $\mathbf{r}_n=nD\mathbf{u}_x=x_n\mathbf{u}_x$ (with n an integer number). For simplicity, we will assume incoming plane waves with wave vector $\mathbf{k}_0\perp\mathbf{u}_z$ (i.e., the fields do not depend on the z coordinate), with $k=\omega/c$ and $\mathbf{k}_0=k\sin\theta\mathbf{u}_x+k\cos\theta\mathbf{u}_y\equiv Q_0\mathbf{u}_x+q_0\mathbf{u}_y$. The reflectance R and transmittance T of the cylinder array can be calculated by using a standard multiple scattering approach in the dipolar approximation,[16] as described in Ref. 17.

We define the absorptivity (=emissivity[1]), A, as $A\equiv 1-R-T$ and the normalized extinction E as the ratio between scattered plus absorbed powers and incoming power (notice that, below the onset of the first diffraction beam, the extinction is simply given by the sum of absorption and specular reflection, $E=A+R$).

Let us first consider the simpler case of *s*-polarized electromagnetic waves (with the electric field parallel to the cylinder axis), $\mathbf{E}=\mathrm{E}(\mathbf{r})\mathbf{u}_z=\mathrm{E}^0e^{iQ_0x}e^{iq_0y}\mathbf{u}_z$. The field scattered from a single subwavelength cylinder n is given by the first (dipolar) term in the Mie expansion for cylindrical waves[18] and can be written as

$$\mathrm{E}_n^{scatt}(\mathbf{r})=\alpha_{zz}\mathrm{E}_{\mathrm{in}}(\mathbf{r}_n)k^2G_0(\mathbf{r},\mathbf{r}_n), \tag{1}$$

where $G_0(\mathbf{r},\mathbf{r}_n)=(i/4)H_0(k|\mathbf{r}-\mathbf{r}_n|)$ is the free-space Green function (H_0 is the Hankel function), $\mathrm{E}_{\mathrm{in}}(\mathbf{r}_n)$ is the incident

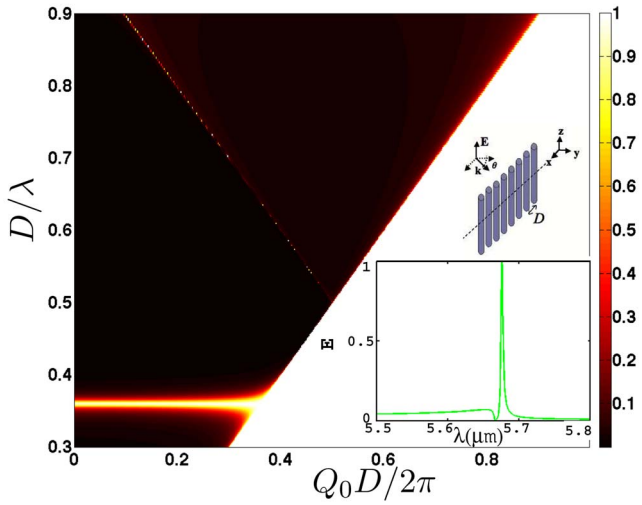

FIG. 1. (Color online) (*s* polarization) Extinction in *s*-polarization in a map of frequency (D/λ) versus the transversal momentum of the incoming radiation ($Q_0=2\pi \sin\theta/\lambda$), for an array of SiC nanocylinders with period $D=4.5$ μm and radius $a=0.2$ μm. Around $D/\lambda=0.36$ ($\lambda=12.5$ μm), there is an isotropic extinction peak due to the absorption line of SiC. The inset shows the extinction spectrum, which exhibits a typical Fano line shape, for an incident angle $\theta=15°$ around the geometric resonance (close to the first Rayleigh frequency, i.e., $D/\lambda=1-Q_0D/2\pi$).

field on the scatterer and, in the small particle limit, the polarizability α_{zz} is given by[19]

$$\alpha_{zz} \approx \pi a^2(\epsilon-1)\left[1-i\frac{\pi}{4}(ka)^2(\epsilon-1)\right]^{-1}. \tag{2}$$

We can write it in the following form:

$$\frac{1}{k^2\alpha_{zz}} = \{C(\epsilon'-1)+\cdots\} - i\left\{\frac{1}{4}+C\epsilon''+\cdots\right\}, \tag{3}$$

where $C^{-1}\equiv\pi(ka)^2|\epsilon-1|^2$. It is worth noticing that $\left(-\mathrm{Im}\{1/(k^2\alpha_{zz})\}-\frac{1}{4}\right)\propto\epsilon''$, so, in absence of absorption ($\epsilon''=0$), the expression above is consistent with the optical theorem.[17,20,21] Multiple scattering effects, due to the presence of the other scatterers, can be included in a renormalized polarizability, $\hat{\alpha}_{zz}$.[17,20] Generalizing the results of Ref. 17 to include absorption we find

$$(k^2\hat{\alpha}_{zz})^{-1} = \mathrm{Re}\left\{\frac{1}{k^2\alpha_{zz}}-G_b\right\} - i\{C\epsilon''+\mathrm{Im}\{G\}\}, \tag{4}$$

where G_b is the depolarization term,[17,20,22] defined as $G_b=\lim_{\mathbf{r}\to\mathbf{r}_0}[G(\mathbf{r})-G_0(\mathbf{r},\mathbf{r}_0)]$, being G the Green function of the periodic array and $\mathrm{Im}\{G\}\equiv\mathrm{Im}\{G(0)\}$.

The absorptivity and normalized extinction can now be written in terms of $\hat{\alpha}_{zz}$ as

$$A^{(s)} = \frac{k^4|\hat{\alpha}_{zz}|^2}{Dq_0}C\epsilon'' \tag{5}$$

$$= \frac{C\epsilon''}{Dq_0}\left[\mathrm{Re}^2\left\{\frac{1}{k^2\alpha_{zz}}-G_b\right\}+\{C\epsilon''+\mathrm{Im}\{G\}\}^2\right]^{-1}, \tag{6}$$

$$E^{(s)} = A^{(s)} + \frac{k^4|\hat{\alpha}_{zz}|^2}{Dq_0}\left(\mathrm{Im}\{G\}-\frac{1}{4Dq_0}\right). \tag{7}$$

In order to illustrate the main physics involved in the different resonant phenomena, we will consider a typical dielectric constant given by $\epsilon=\epsilon_\infty(\omega_L^2-\omega^2-i\gamma\omega)\{\omega_T^2-\omega^2-i\gamma\omega\}^{-1}$. This is a standard form for a polar material (Lorentz model), with ω_T and ω_L, the frequencies of the transverse and the longitudinal mode of optical phonons, respectively. For a metal, the Drude model is recovered taking $\omega_T=0$ and $\omega_L=\omega_p$. Silicon carbide (SiC) nanowires provide a simple model system: its dielectric constant is given by this form with the following parameters:[23] $\epsilon_\infty=6.7$, $\omega_L=1.825\times10^{14}$ rad s^{-1}, $\omega_T=1.494\times10^{14}$ rad s^{-1}, $\gamma=8.9662\times10^{11}$ rad s^{-1}.

Figure 1 displays the extinction in the infrared range, in a map of frequency (D/λ) versus the transversal momentum of the incoming radiation (Q_0), for an array of SiC cylinders (with $D=4.5$ μm and $a=0.2$ μm). The extinction spectra show two different kinds of resonances: (i) close and below the Rayleigh frequency $\omega\to\omega_1^{(-)}=c|Q_0-2\pi/D|$ the spectra present a very sharp peak with a strong dependence on the angle of incidence, and (ii) a broad peak close to the absorption line of SiC ($\omega\approx\omega_T$) which is almost isotropic. The peaks in the extinction spectra correlate with corresponding maxima in the absorption. However, the relative strength of the peaks depends on the material and geometrical parameters. This is illustrated in Fig. 2 where we have plotted the real part of $1/\alpha_{zz}$ and the imaginary parts of α_{zz} [Fig. 2(a)], the absorptivity [Fig. 2(b)] and the extinction [Fig. 2(c)] versus the wavelength for an incident angle $\theta=15°$ an for different lattice constants, D [the inset in Fig. 1 corresponds to a zoom of the bold solid line in Fig. 2(c)].

The different extinction/absorption resonances resemble the recently discussed "lattice"[17,24] and "site"[25] resonances in absence of absorption. The resonance takes place when

$$\mathrm{Re}\{1/(k^2\alpha_{zz})-G_b\}=0. \tag{8}$$

Approaching the threshold of the first propagating (diffraction) channel, the real part of G_b goes to infinity as $\approx(\omega_1^2-\omega^2)^{-1/2}c/(2D)$ and can compensate exactly the real part of $1/k^2\alpha_{zz}$ giving rise to a "geometric" resonance.[17,20] This can only happen when the real part of the polarizability is positive ($\epsilon'>1$). As a consequence, in *s* polarization there is no resonant absorption for metallic cylinders. The typical Fano line shape of these resonances is illustrated in the inset of Fig. 1. We can also notice that exactly at the Rayleigh frequency, $\omega=\omega_1$, the array of cylinders is transparent as the absorption and the extinction goes to zero.

Sharp peaks in Figs. 2(b) and 2(c) correspond to geometric resonances appearing just below the threshold of a new propagating order. For example, in the extinction spectra of Fig. 2(c) the three sharp peaks observed for $D=11$ μm (blue dashed lines) correspond to the Rayleigh frequencies for the $m=2$ order at $\lambda=6.92$ μm, $m=-1$ order at $\lambda=8.15$ μm and the $m=1$ order at $\lambda=13.84$ μm.

While it is possible to obtain a 100% extinction of the beam (due to the reflection resonances which appear when

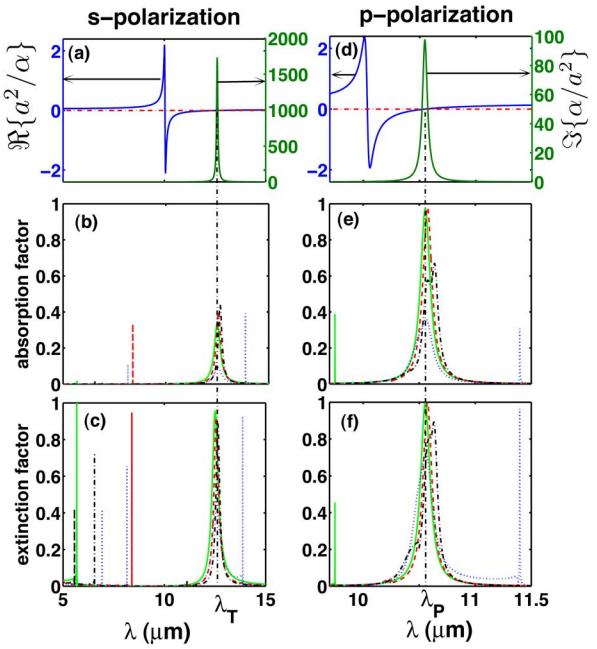

FIG. 2. (Color online) (*s* polarization) (a) Real part of $1/\alpha_{zz}$ and imaginary part of α_{zz} versus λ for SiC cylinders. Absorption resonance is due to a zero (–·–) of $\mathrm{Re}\{1/\alpha_{zz}\}$, which coincides with a maximum of $\mathrm{Im}\{\alpha_{zz}\}$. (b) Absorption spectrum versus λ for arrays of cylinder of radius $a=0.2$ μm, for an incident angle $\theta=15°$ and for several periods $D=4.5$ μm (green bold solid line), $D=6.67$ μm (red dashed line), $D=8.83$ μm (black dotted-dash line), $D=11$ μm (blue dotted line). (c) Extinction spectrum for the same parameters as (b). (*p* polarization) (d) Real part of $1/\alpha_p$ and imaginary part of α_p versus λ for SiC cylinders. (e) Absorption spectrum versus λ for arrays of cylinders of radius $a=0.5$ μm and different periods $D=5.71$ μm (green solid line), $D=6.0$ μm (red dashed line), $D=6.15$ μm (black dotted-dash line), $D=6.667$ μm (blue dotted line), (f) Extinction spectrum for the same parameters as (e).

the absorption is weak[17]), the maximum absorption A_{max} is limited to 50% [see Figs. 2(b) and 2(c)]. It is easy to show that the highest absorption, $A_{max}=1/2$, takes place below the first Rayleigh frequency when

$$C\epsilon'' = \frac{\epsilon''}{\pi(ka)^2|\epsilon-1|^2} = \frac{1}{2Dq_0}. \tag{9}$$

This is one of the central results of this work.

Material or "site" resonances are associated to the zeros of the real part of $1/\alpha_{zz}$. As shown in Fig. 2(a), it exhibits two zeros, one close to $\omega \simeq \omega_T$ the other to $\omega^2 \simeq \omega_S^2 = (\epsilon_\infty \omega_L^2 - \omega_T^2)/(\epsilon_\infty - 1)$. The second one corresponds to a small value of $\mathrm{Im}\{\alpha_{zz}\}$, which leads to a weak absorption. The broad resonances in Figs. 2(b) and 2(c) coincide with a maximum of $\mathrm{Im}\{\alpha_{zz}\}$ and correspond to a resonant absorption of the material due to the excitation of the transverse mode of optical phonons (for $\lambda_T=12.61$ μm).

Then, they should not be very sensitive to the lattice parameters and order. However, the maximal absorptivity value of 1/2 can only be reached at the condition given by Eq. (9).

III. ANALYTICAL STUDY FOR *p* POLARIZATION

Let us now consider an incoming wave with the magnetic field parallel to the cylinder axis (*p*-polarized wave). Following the notation of Ref. 17 we can now define the renormalized polarizabilities of the effective dipoles pointing along the *x* and *y* axis: $\hat{\alpha}_{xx}=(1+\alpha_{xx}\partial_y^2 G_b)^{-1}\alpha_{xx}$, $\hat{\alpha}_{yy}=(1+\alpha_{yy}\partial_x^2 G_b)^{-1}\alpha_{yy}$, with $\partial_{x,y}^2 G_b$ being the depolarization terms due to the components *x* and *y* of the electric field scattered by all the dipoles (except the considered one) and $\alpha_{xx}=\alpha_{yy}=\alpha_p$ the polarizability of a cylinder in *p* polarization,

$$\frac{1}{k^2\alpha_p} = \left\{\frac{C}{2}(|\epsilon|^2-1)+\cdots\right\} - i\left\{\frac{1}{8}+C\epsilon''+\cdots\right\}. \tag{10}$$

The general expression for the absorption is

$$A^{(p)} = \frac{k^2}{Dq_0}(Q_0^2|\hat{\alpha}_{yy}|^2 + q_0^2|\hat{\alpha}_{xx}|^2)C\epsilon''. \tag{11}$$

Hence, in *p* polarization, the absorption results from the sum of the contributions of two dipoles, one pointing in the *x* direction (with an effective polarizability $\hat{\alpha}_{xx}$) and one pointing in the *y* direction (with an effective polarizability $\hat{\alpha}_{yy}$). We now have different resonance conditions for each dipole, respectively in the *x* and *y* direction:

$$\mathrm{Re}\{1/\alpha_p - \partial_y^2 G_b\} = 0, \tag{12}$$

$$\mathrm{Re}\{1/\alpha_p - \partial_x^2 G_b\} = 0. \tag{13}$$

At the threshold of the first propagating order, there is a resonant coupling of electric dipoles pointing along the *y* axis which leads to the divergence of $\mathrm{Re}\{\partial_x^2 G_b\} \approx -(\omega_1^2-\omega^2)^{-1/2}\omega_1^2/(2cD)$ at the Rayleigh frequencies (in contrast $\mathrm{Re}\{\partial_y^2 G_b\}$ remains finite). Close to the first Rayleigh anomaly ($\omega \lesssim \omega_1$) and providing that $\mathrm{Re}\{1/\alpha_p\}>0$,[17] the absorption contains two parts: a resonant part due to the resonance of $\hat{\alpha}_{yy}$ (and similar to the case in *s* polarization), and the term due to $\hat{\alpha}_{xx}$ to which we will refer as a "background contribution."

For *p* polarization, the resonant part has also a maximal value of 1/2 and reaches this maximum when

$$C\epsilon'' = \frac{Q_0^2}{k^2}\frac{1}{2Dq_0}. \tag{14}$$

Depending on the contribution of the nonresonant part, the absorption can reach a value higher than 1/2.

Site resonances for *p* polarization are again associated to zeros of the real part of $1/\alpha_{xx}=1/\alpha_{yy}=1/\alpha_p$. $\mathrm{Re}\{1/\alpha_p\}$ exhibits two zeros [see Fig. 2(d)]: one close to $\omega \simeq \omega_S$, but corresponding to a small value of $\mathrm{Im}\{\alpha_p\}$ and to $\epsilon'=+1$ and thus a weak absorption (for SiC, $\lambda_S=10.0$ μm), the other close to $\omega \simeq \omega_P$ ($\epsilon' \approx -1$) which gives rise to (phonon polaritons or plasmon polaritons for metals) LSPR (for SiC, $\lambda_P=10.57$ μm). When $\omega \simeq \omega_P$, with an appropriate choice of geometrical parameters it is possible to match the two resonance conditions [Eqs. (12) and (13)]. In contrast with the geometric resonances, the LSPR will lead to the resonance of both dipoles and, as each dipole can contribute up to 1/2, the absorption may reach 100%.

We have to notice the frequency of the plasmon resonances are shifted by the real part of the depolarization terms, $\mathrm{Re}\{\partial_x^2 G_b\}$ for the dipole pointing along the y axis and $\mathrm{Re}\{\partial_y^2 G_b\}$ for the dipole pointing along the x axis [Eqs. (12) and (13)]. Hence, unless $\mathrm{Re}\{\partial_x^2 G_b\}=\mathrm{Re}\{\partial_y^2 G_b\}$, the two effective dipoles will not resonate exactly at the same frequency, thus this value of the absorption maximum will be very sensible to the lattice parameters. Together with this condition, it can be easily shown that the other condition to reach the maximal absorption is $q_0=Q_0(\theta=45°)$. We represent in Figs. 2(e) and 2(f), respectively, the absorption and extinction spectra of an array of SiC cylinders with a radius of $a=0.5$ μm and for an incident angle of $\theta=45°$ and several periods. Similarly to s polarization, there are two kinds of resonances, (1) geometric resonance characterized by very sharp peaks at wavelengths close to Rayleigh frequencies, and (2) a broader peak at a wavelength $\lambda \simeq \lambda_P$.

As the resonant condition is different for each dipole [Eqs. (12) and (13)], depolarization effects lead to a splitting of the plasmon peak. This *double peak* in the absorption and extinction spectra corresponds to the resonances of the y and x dipoles, (red or blue) shifted depending on the sign $(+$ or $-)$ of $\partial_x^2 G_b$ and $\partial_y^2 G_b$. As discussed above, $\approx 100\%$ absorption takes place only when $\partial_x^2 G_b \approx \partial_x^2 G_b$. It is worth noticing that in the wavelength range where $\mathrm{Re}\{1/\alpha_p\}<0$ (i.e., $|\epsilon|<1$), there are no geometric resonances. This explains the anomalous shape of the LSPR extinction peak for $D=6.15$ μm [black dotted-dashed line in Fig. 2(f)], as the Rayleigh frequency ($\lambda=10.5$ μm) lies in a range where $\mathrm{Re}\{1/\alpha_p\} \lesssim 0$. At this wavelength, we can just observe the (y dipole) Rayleigh transparency dip in the extinction spectrum (see also Fig. 3). These results provide a simple and analytical explanation of the anomalous shape of the extinction peaks observed in recent numerical simulations.[10]

IV. CONCLUSION

In conclusion, this paper gives a simple analytical method to derive the optical properties of subwavelength cylinders arrays. We have shown that in s polarization, absorption resonances can absorb up to half of the incident power. The absorption and extinction spectra for p polarization presents a more complex structure due to the contribution of two orthogonal dipoles. It is remarkable that, as we have shown, by an appropriate choice of parameters a subwavelength cylinder array can become a perfect absorber. We believe that our analysis paves a way for the nanoengineering of chemical and biological sensors and photothermal devices based on nanoparticle arrays.

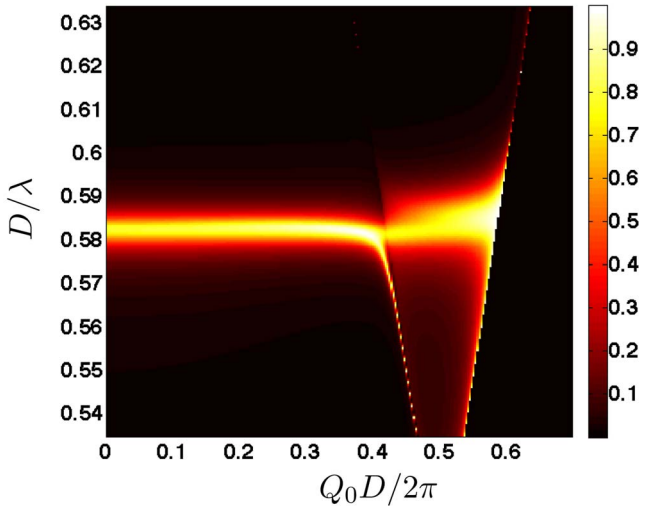

FIG. 3. (Color online) (p polarization) Extinction map for an array of SiC cylinders with a period $D=6.15$ μm, a radius of $a=0.5$ μm. The localized surface phonon-polaritons resonance, at the wavelength $\lambda \simeq \lambda_P$, is isotropic.

ACKNOWLEDGMENTS

We thank J. García de Abajo and O. J. F. Martin for interesting discussions. This work has been supported by the Spanish MEC (Ref. No. EX2005-1181), the EU Integrated Project "Molecular Imaging" (EU contract LSHG-CT-2003-503259), and the EU network of excellence "Plasmo-nano-device" (FP6-2002-IST-1-507879).

*URL: http://www.uam.es/mole

[1] See for example, F. Reif, *Fundamentals of Statistical and Thermal Physics* (McGraw-Hill, New York, 1965), Chap. 9; J.-J. Greffet and M. Nieto-Vesperinas, J. Opt. Soc. Am. A **15**, 2735 (1998); C. Y. Luo, A. Narayanaswamy, G. Chen, and J. D. Joannopoulous, Phys. Rev. Lett. **93**, 213905 (2004).

[2] S. Y. Lin, J. G. Fleming, E. Chow, J. Bur, K. K. Choi, and A. Goldberg, Phys. Rev. B **62**, R2243 (2000).

[3] S. Enoch, J.-J. Simon, L. Escoubas, Z. Elalmy, F. Lemarquis, P. Torchio, and G. Albrand, Appl. Phys. Lett. **86**, 261101 (2005).

[4] V. Yannopapas, Phys. Rev. B **73**, 113108 (2006).

[5] M. Laroche, R. Carminati, and J.-J. Greffet, Phys. Rev. Lett. **96**, 123903 (2006).

[6] J.-J. Greffet, R. Carminati, K. Joulain, J. P. Mulet, S. Mainguy, Y. Chen, Nature (London) **416**, 61 (2002).

[7] M. Laroche, C. Arnold, F. Marquier, R. Carminati and J.-J. Greffet, S. Collin, N. Bardou, and J.-L. Pelouard, Opt. Lett. **30**, 2623 (2005).

[8] B. Lamprecht, G. Schider, R. T. Lechner, H. Ditlbacher, J. R. Krenn, A. Leitner, and F. R. Aussenegg, Phys. Rev. Lett. **84**, 4721 (2000); N. Félidj, J. Aubard, G. Levi, J. R. Krenn, G. Schider, A. Leitner, and F. R. Aussenegg, Phys. Rev. B **66**, 245407 (2002).

[9] Q.-H. Wei, K.-H. Su, S. Durant, and X. Zhang, Nano Lett. **4**, 1067 (2004).

[10] S. Zou, N. Janel, and G. C. Schatz, J. Chem. Phys. **120**, 10871 (2004); E. M. Hicks, S. Zou, L. Gunnarsson, T. Rindzevicius, M. Käll, B. Kasemo, G. C. Schatz, K. G. Spears, and R. P. Van

Duyne, Nano Lett. **5**, 1065 (2005).
[11] M. S. Anderson, Appl. Phys. Lett. **83**, 2964 (2003).
[12] A. N. Shipway, E. Katz, and I. Willner, ChemPhysChem **1**, 18 (2000).
[13] J. P. Kottmann, O. J. F. Martin, D. R. Smith, and S. Schultz, Phys. Rev. B **64**, 235402 (2001); J. P. Kottmann, O. J. F. Martin, D. R. Smith, and S. Schultz, Opt. Express **6**, 213 (2000).
[14] S. J. Oldenburg, R. D. Averitt, S. L. Westcott, and N. J. Halas, Chem. Phys. Lett. **288**, 243 (1998).
[15] H. Rigneault, F. Lemarchand, A. Sentenac, and H. Giovannini, Opt. Lett. **24**, 148 (1999); A. L. Ferhembach and A. Sentenac, Appl. Phys. Lett. **86**, 121105 (2005).
[16] L. Foldy, Phys. Rev. **67**, 107 (1945); M. Lax, Phys. Rev. **85**, 621 (1952); V. Twersky, J. Opt. Soc. Am. **52**, 145 (1962); K. Ohtaka and H. Numata, Phys. Lett. **73A**, 411 (1979).
[17] R. Gómez-Medina, M. Laroche, and J. J. Sáenz, Opt. Express **14**, 3730 (2006).
[18] See, for example, C. F. Bohren and D. R. Huffman, *Absorption and Scattering of Light by Small Particles*, Sec. 8.4 (Wiley, New York, 1998).
[19] B. T. Draine, Astrophys. J. **333**, 848 (1988).
[20] R. Gómez-Medina and J. J. Sáenz, Phys. Rev. Lett. **93**, 243602 (2004).
[21] V. A. Markel, J. Chem. Phys. **122**, 097101 (2005).
[22] M. Meier, A. Wokaun, and P. F. Liao, J. Opt. Soc. Am. B **2**, 931 (1985).
[23] E. D. Palik, *Handbook of Optical Constants of Solids* (Academic, San Diego, 1985).
[24] F. J. García de Abajo, R. Gómez-Medina, and J. J. Sáenz, Phys. Rev. E **72**, 016608 (2005).
[25] F. J. García de Abajo, and J. J. Sáenz, Phys. Rev. Lett. **95**, 233901 (2005); F. J. García de Abajo, J. J. Sáenz, I. Campillo, and J. S. Dolado, Opt. Express **14**, 7 (2006).